Discover Soil

Research

Soil CO_2 and CH_4 response to experimental warming under various tree species compositions in a temperate harwood forest

Sharlène Laberge[1,2] · Blandine Courcot[1,2] · Rolando Trejo-Pérez[1,2] · Nicolas Bélanger[1,2]

Received: 6 September 2024 / Accepted: 19 February 2025
Published online: 11 March 2025
© The Author(s) 2025 OPEN

Abstract
Under climate change, some forest ecosystems appear to be transitioning into net source of carbon dioxide (CO_2), raising questions about the future role of soil respiration rate (R_s), which depends on hydroclimatic conditions. Conversely, well-drained forest soils could become more significant sinks of methane (CH_4) under warming. The main objective of this study was to assess the effects of artificial soil warming on R_s and CH_4 fluxes in a sugar maple forest at the northern limit of Quebec temperate deciduous forests in eastern Canada, and to evaluate the effect of species composition on soil response to warming. We measured R_s and CH_4 fluxes during the snow-free period of 2021 and 2022 in 32 plots distributed across three forest types, half of which were artificially heated by approximately 2 °C with heating cables. Forest soils were a very consistent sink for CH_4 and it did not respond to artificial soil warming nor was it sensitive to variations in soil moisture, ionic activity in soil solution and forest types. However, we observed an increase in R_s in response to warming in the heated plots, but only up to a threshold of about 15 °C, beyond which R_s started to slow down in respect to the control plots. We also observed a weakening of the exponential relationship between R_s and soil temperature beyond this threshold. This trend varied across the forest types, with hardwood-beech stands being more sensitive to warming than mixedwoods and other hardwoods. This greater response of hardwood-beech stands to warming resulted in a more significant downshift of R_s, starting from a colder temperature threshold, around 10–12 °C. This study highlights a potential plateauing of R_s despite rising soil temperature, at least in eastern Canada's temperate deciduous forest, but this trend could vary from one forest type to another.

Keywords Temperate forest · Soil respiration · Methane · Artificial warming · Drying · Species composition

1 Introduction

Soils are an important component of the global carbon cycle as they represent the largest terrestrial carbon reservoir and produce, through respiration, the second-largest carbon dioxide (CO_2) flux after plant photosynthesis [1]. Soil respiration (R_s) consists of autotrophic respiration, which includes root and rhizosphere respiration, and heterotrophic respiration, which involves organic matter decomposition by soil communities [2]. Soil respiration is mostly influenced

Supplementary Information The online version contains supplementary material available at https://doi.org/10.1007/s44378-025-00045-4.

✉ Nicolas Bélanger, nicolas.belanger@teluq.ca | [1]Data Science Laboratory, Université du Québec (TELUQ), Montreal, QC, Canada. [2]Centre d'étude de la forêt, Université du Québec à Montréal, Montreal, QC, Canada.

by soil hydroclimatic conditions, namely temperature and water content [3], as well as secondary factors such as species composition, which influences soil hydroclimatic conditions [4, 5].

Soil temperature is the variable that best explains the spatiotemporal variations in R_s [6, 7]. Except for certain ecosystems such as deserts, an increase in soil temperature leads to an increase in R_s [8]. Specifically, the relationship between soil temperature and R_s is positive and curvilinear, as demonstrated by several studies focusing on the influence of soil temperature on R_s in temperate forests [9, 10]. Soil temperature sensitivity is generally described by the Q_{10} value, which is the coefficient of the exponential relationship between R_s and temperature, multiplied by 10 [11]. Seasonal variations in R_s in ecosystems characterized by seasonality are however not solely attributable to temperature changes. At certain times of the year, the relationship between temperature and R_s is confounded by soil moisture [12] and phenology [13, 14].

During periods of drought, soil moisture becomes a limiting factor [15, 16]. Soil drying induced by warming and increased evaporative demand can thus explain the gradual decrease in soil sensitivity to increasing temperature that may be observed [17]. However, while the relationship between temperature and R_s is generally exponential, the relationship between moisture and R_s is more complex. Microbial activity, and therefore heterotrophic respiration, reaches a maximum within a certain range of soil water content [1]. The net effect of soil warming on R_s thus depends on the balance between the influence of temperature and soil moisture [18, 19]. Forest species composition may also influence R_s because it modulates (1) root activity, (2) soil chemical properties, such as nutrient availability and acidity, (3) litter inputs and quality, (4) microclimate, and (5) microbial communities and activity [4, 5, 9].

In the context of climate change and increasing droughts and fires, forest ecosystems transitioning to net sources of CO_2 are increasing, including some forested regions that are not adapted to drought and fire [20, 21]. In such context, the role of R_s on atmospheric CO_2 concentration is uncertain. While R_s could intensify because of warmer conditions, it could also decrease because of increased droughts and decreased net primary productivity, or it could remain unchanged because changes in temperature and moisture may offset each other [17, 22, 23]. Several studies reported tree growth decline and forest dieback in boreal and temperate ecosystems due to droughts [24–27]. Recurrent exposure to water stress can however promote ecological memory mechanisms that make trees more resilient to extreme climatic events [28, 29]. Species that recover more quickly from drought are likely to be favored under climate change with a greater frequency and intensity of water stress events. For example, Hesse et al. [30] showed that European beech (*Fagus sylvatica* L.) physiologically recovers more quickly following water stress events than Norway spruce (*Picea abies* (L.) Karst.). Similarly, since drought legacy is modulated by species composition, some forest types may have a greater capacity to resist to changes in soil microclimate under extreme weather events than others [31–33]. Canarini et al. [34] proposed that cumulative drought can increase soil resilience by promoting their multifunctionality (e.g., microbial activity). However, the relationships between forest species composition, soil microclimate, high water stress, soil memory, and R_s remain to be elucidated.

Conversely, well-drained (upland) forest soils generally act as a considerable sink for atmospheric CH_4 due to the presence/activity of methane-oxidizing bacteria, i.e., aerobic methanotrophs [35–37]. Like R_s, methanotrophic processes have been linked to: (1) environmental conditions (e.g., soil temperature) and plant species composition which affect bacterial communities and activity, (2) soil moisture and winter conditions (e.g., snow cover, freeze–thaw) which affect bacteria and CH_4 transport in the soil, and (3) particle size distribution which affects CH_4 transport [36]. On the one hand, decreases in atmospheric nitrogen deposition [38] and increases in atmospheric CH_4 concentrations [39] should explain the increase in CH_4 uptake by forest soils observed in some studies [40]. On the other hand, a decrease in the strength of the CH_4 sink (between about 50–75%) was also observed since the late 1990s in eastern North America forest sites and elsewhere [37]. This decrease in the CH_4 sink of forest soils is believed to be due to increases in precipitation and thus a greater soil water flux. Experimental warming studies in forest soils suggest only small and temporary (short-lived) effects on CH_4 fluxes, mostly increasing the sink's strength [41, 42] but occasionally decreasing it [43]. However, the long-term effects of warming on CH_4, through affectation of a series of variables such as soil moisture, carbon, nitrogen and microbes, are poorly understood [43, 44]. Considering that CH_4 is the second-most important greenhouse gas after CO_2 and on a significant upward trend regarding anthropogenic emission rates and atmospheric concentrations [45], elucidating the direct and indirect effects of warming on CH_4 dynamics in forest soils is needed for a robust estimation of the contribution of this greenhouse gas sink in the long term.

The objective of this research was to assess the short-term effects of artificial soil warming on R_s and CH_4 fluxes across a range of forest plots that encompass differences in the prevalence of conifers and American beech (*Fagus grandifolia* Ehrh.) within the northern range limit of Quebec temperate deciduous forest. It was hypothesized that artificial soil warming would generally lead to an increase in R_s in both mixedwoods and hardwoods, except during the warmest periods

of summer when R_s would slow down due to a decrease in its temperature sensitivity following drying and water stress induced by increased evaporative demand. It was also hypothesized that artificial soil warming would slightly increase the CH_4 sink, mainly because of some soil drying. Finally, it was hypothesized that the effects of artificial drying on R_s would be smaller in plots where beech is abundant because it tends to protect soils from droughts [33]. A better understanding of the relationships between forest species composition and soil processes can better guide decision-making in forestry that aims at making forests more resilient to climate change as well as using them as an efficient natural climate solution.

2 Materials and methods

2.1 Study site

The study took place at the Station de Biologie des Laurentides of Université de Montréal in Saint-Hippolyte, Quebec (45°59′17″N, 74°00′20″W), which is located at the northern limit of the maple-yellow birch bioclimatic domain [46]. The site is mostly composed of sugar maple (*Acer saccharum* Marsh.), red maple (*Acer rubrum* L.), American beech (*Fagus grandifolia* Ehrh.), yellow birch (*Betula alleghaniensis* Britton), white birch (*Betula papyrifera* Marshall), eastern white cedar (*Thuja occidentalis* L.), white pine (*Pinus strobus* L.), and large-tooth aspen (*Populus grandidentata* Michx.) [47]. Due to its proximity to the boreal forest, species that are typical of that biome, notably balsam fir (*Abies balsamea* (L.) Mill.), are also present. The average temperature at the study site is 4.3 °C, while the average precipitation is 1195 mm, with 900 mm of rain and 297 cm of snow [9]. Soils are orthic humo-ferric and ferro-humic podzols [48] that developed from a well-drained glacial till with a loamy sand texture [49]. The forest floor is of the moder type, although the mor type can be found in wetter areas dominated by cedar.

2.2 Experimental design

The experimental design consisted of eight stands distributed across three distinct zones. Based on basal area and forest floor litter data, Bélanger et al. [9] classified stands into three forest types: mixedwoods, hardwoods, and hardwood-beech stands (Table 1). Stands were classified as mixedwoods when the basal area of balsam fir represented more than 20% of the total basal area. Hardwoods and hardwood-beech stands were differentiated based on the contribution of beech litter to the total litter. If beech litter accounted for more than 20% of the total forest floor litter in a stand, it was classified as a hardwood-beech stand, and if it was accounted for less than 20% of the total litter, it was classified as a hardwood. The litter was also collected in autumn 2021 as part of this study, and the results obtained (Table 1) were very similar to those collected by Bélanger et al. [9] between 2017 and 2020, suggesting that forest types had not changed significantly (e.g., from a disturbance such as windthrow). Thus, the original forest type classification was maintained. There were two forest types in zone 1 (mixedwoods and hardwoods), two types in zone 2 (mixedwoods and hardwood-beech stands), and

Table 1 Description of experimental design by zone, forest type and tree species contributions to total litterfall mass in each stand

Zone	Stand	Forest type	Contribution (%)						
			Leaves	Needles	AS	AR	Betula	FG	PG
1	1	Mixedwood	67.6	32.5	3.97	47.4	16.2	0	0
1	2	Hardwood	99.2	0.71	70.9	19.4	5.93	0	2.92
2	3	Hardwood-beech	99.9	0	60.1	12.8	6.44	20.6	0
2	4	Mixedwood	84.5	15.6	72.4	0	6.78	5.28	0
3	5	Hardwood-beech	99.7	0.35	51.3	0	31.8	16.6	0
3	6	Hardwood	98.7	1.23	52.3	15.1	19.9	11.4	0
3	7	Mixedwood	99.5	0.42	39.0	53.2	1.56	1.76	3.96
3	8	Hardwood-beech	99.9	0	46.1	37.1	0.75	16.0	0

N.B. Litter was collected in autumn 2021, but the classification of stands by forest type is based on Bélanger et al. [9]. The values in italics indicate that the data in this study differed slightly from the ones in Bélanger et al. [9] in respect to the > 20% criterion for classification of hardwood-beech stands. AS is *Acer saccharum* (sugar maple), AR is *Acer rubrum* (red maple), Betula is *Betula alleghaniensis* and *Betula papyrifera* (yellow birch and white birch), FG is *Fagus grandifolia* (American beech) and PG is *Populus grandidentata* (large-tooth aspen). Needles mostly come from *Abies balsamea* (balsam fir)

all three types in zone 3. Due to the challenges of electrifying forest stands, not all zones included all three forest types. The experimental design was therefore unbalanced with respect to the distribution of forest types among zones. In May 2022, a major windstorm changed species composition significantly by toppling all mature fir trees. This event led to a 5-day power outage as well as a large opening in the canopy, thus providing significantly more light to the forest floor.

For the soil warming treatment, the heating cable method was preferred because it is relatively simple to set up when power is available, and it allows to create a considerable temperature differential with relatively high precision [50]. Each stand consisted of four 3 × 3 m plots, including two control plots and two plots artificially heated using twin conductor 120 V heating cables (RX Roof & Gutter De-Icing Cables, Danfoss). In the heated plots, 36 m of cables were buried in a slalom pattern (~ 15 cm spacing) in May 2017 at a depth of about 12 cm, which corresponds to the forest floor and mineral soil interface. Soils were heated for 15 min every hour over 24 h using mechanical timers starting only for one month toward the end of 2020 (i.e., mid-October to mid-November). The warming treatment was then applied during the snow-free period of 2021 and 2022, from mid-April to mid-November, thus extending the biologically active period by 4–6 weeks. The mechanical timer method has the advantage of providing an equal amount of energy in each plot and avoiding imprecision associated with electronic systems due to the installation of reference probes at various/inconsistent distances from the heating cables [51]. Each plot was equipped with two temperature probes (Spectrum Technologies) and two soil water potential probes (Watermark 200SS Sensor, Irrometer), all connected to a WatchDog 1650 Micro Station (Spectrum Technologies) that logged data at 30-min intervals. All probes were placed near the center of two rows of heating cable. The warming treatment created a consistent temperature differential of approximately 2 °C for all three forest types (Fig. 1). Soil water potential is typically expressed in negative values, meaning that as the soil dries, the water potential becomes more negative. However, for simplicity, soil water potential is thereafter expressed in positive values. A more positive water potential value thus means a drier soil, whereas a water potential close to zero indicates a wet soil. Unfortunately, problems with dataloggers in 2021 due to large changes in air temperature and thus condensation in the spring led to some gaps in soil climate data that limited analyses. This problem was completely resolved in 2022.

2.3 Field and laboratory methods

Gas samples at the soil-atmosphere interface were collected before the artificial warming in 2019 and 2020 by Bélanger et al. [9], as well as after the onset of the warming treatment in 2021 and 2022 (this study). Soil respiration from the heated plots in 2021 and 2022 could therefore be compared to temporal controls, which correspond to R_s measured by Bélanger et al. [9] in all plots in 2019 and 2020 (i.e., before the onset of warming). Soil respiration from the heated plots could also be compared to spatial controls, which correspond to R_s measured in this study in control plots in 2021 and 2022 (i.e., after the onset of warming). Investigation of CH_4 data in such a way was prevented by the absence of calibrated CH_4 data in 2019 and 2020.

It was considered that the effects of cable installation on soil processes and properties disappeared rapidly (within 1–2 years) and thus, no trenches were dug in the control plots in 2017 to simulate disturbances during cable installation. This was based on literature [52–54] which suggests a lag time of approximately 6–12 months between cable implementation and activation [50] and verified using Plant Root Simulator (PRS) probes (Western Ag Innovations) which measure the ionic activity of soil solutions (unpublished data, N. Bélanger). Sampling was done every two weeks during the snow-free period of 2021 and weekly during the snow-free period of 2022 following the same protocol as in Bélanger et al. [9]. Insulated and ventilated chambers equipped with an Interlink IV injection site (Baxter) were placed on four collars that were installed in each plot in May 2017 (chamber volume of 4.56 L with the collar). Gas was sampled over 20 min at 5-min intervals (t_0, t_5, t_{10}, t_{15}, t_{20}) using a 20 mL syringe equipped with a 25-gauge 5/8-inch needle. Five mL of gas was extracted from each chamber at each time point, for a total of 20 mL. This cumulative sampling technique allows to capture spatial variability in CO_2 flux within the plot [55]. The collected samples were then transferred into vacuumed and sealed 12 mL Exetainer vials (LabCo). Soil temperature and water potential readings were made at the same time as soil CO_2 gas sampling. For each stand, air temperature, relative humidity and pressure were measured at the time of sampling using proper probes and a WatchDog 1650 Micro Station (Spectrum Technologies).

The gas in the vials was analyzed within 48 h after sampling using cavity ring-down (CRD) spectroscopy (G2201-i isotopic gas analyzer, Picarro). The sample gas was carried with an autosampler (OpenAutoSampler) using ultra-zero air. Before analysis, the water vapor from gas samples was removed using a monotube NafionTM gas dryer (PermaPure).

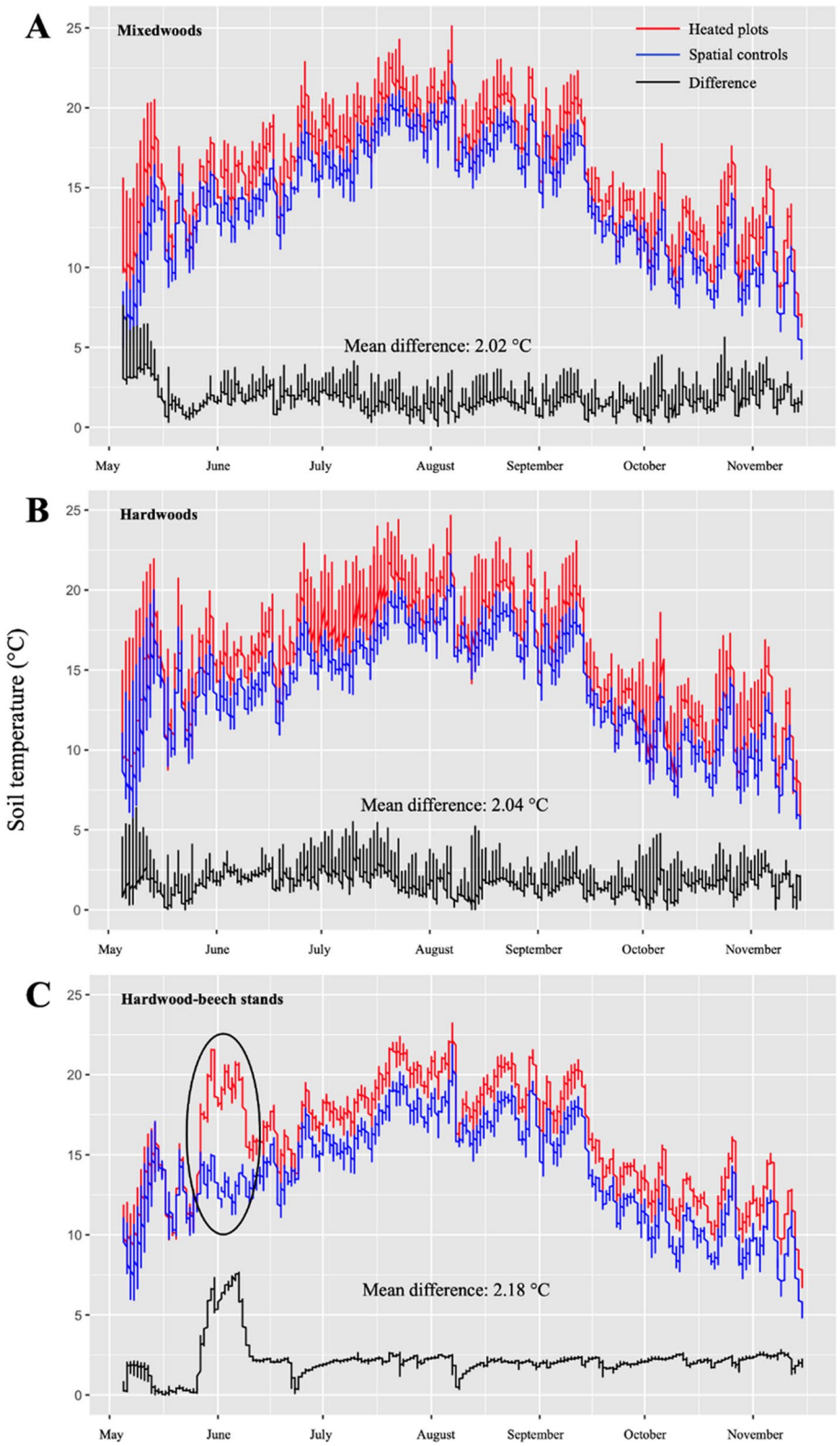


Fig. 1 Seasonal variations in soil temperature from May to October 2022 for the heated plots and spatial controls as well as the average temperature difference between treatments for mixedwoods (**A**), hardwoods (**B**), and hardwood-beech stands (**C**). N.B. The circled region in the hardwood-beech stands corresponds to abnormal soil temperature values in the heated plots. This June anomaly is attributed to a problem with the mechanical timer in stand 8 following the power outage that occurred after a major windstorm in May. This problem was identified and fixed within two weeks.

Carbon dioxide and CH_4 concentrations were then analyzed for each time point. From these concentration values (ppm), CO_2 and CH_4 fluxes (mg m^{-2} h^{-1}) were estimated using the HMR package in R, which fits the data from t_0 to t_{20} to a linear model [56]. The linear model was selected as it provided the best fit for 95% of the collected gas flux samples and led to

consistent results for the remaining 5% [57–59]. This procedure follows the analytical protocol used in Bélanger et al. [9] so that temporal controls could be used as a reliable reference.

During the summers of 2021 and 2022, soil ionic activity (NO_3^-, NH_4^+, SO_4^{2-}, Ca^{2+}, Mg^{2+}, K^+, $H_2PO_4^-$, Al^{3+}, Fe^{3+}, and Mn^{2+}) was measured in each of the plots as a proxy for nutrient availability. One set of four cation and one set of four anion PRS probes were incubated in each plot for 5 weeks, from June 2 to July 14 in 2021 and from June 8 to July 20 in 2022, at a depth of up to 15 cm. Following the incubation period, the probes were removed and cleaned with deionized water and then stored in the fridge until ion extraction. Probes were eluted for 1 h with 0.5 M HCl. The NO_3^- and NH_4^+ ions were analyzed by colorimetry (Autoanalyser III, Bran and Luebbe), whereas other ions extracted from PRS probes were analyzed as their total elementary concentration (sulfur, calcium, magnesium, potassium, phosphorus, aluminum, iron and manganese) by inductively coupled plasma atomic emission spectrometry (ICP-OES, Optima 3000-DV, PerkinElmer). The use of PRS probes is now common in forest ecology [60, 61]. Unlike conventional extraction methods that indicate nutrient availability in the soil at a specific moment only, PRS probes capture the dynamics of soil ionic activity over time.

2.4 Data analysis

Data collected by Bélanger et al. [9], as well as those collected during the summer of 2021 and 2022 (this study), were analyzed using standard packages in R. Variables were first transformed by taking the square root (^1/2) to ensure normal distribution. Statistical testing of the treatment and forest type effects on R_s and CH_4 were first conducted. The block effect was initially tested using a linear mixed model. No blocking effect was detected, which led to testing the effects of treatment and forest type on R_s and CH_4 and their interaction (treatment × forest type) using two-way ANOVA. Two-way ANOVA was conducted on all data as well as on several sets of data which represented several temperature intervals (i.e. 2.5 °C, 5 °C, 10 °C and 15 °C groupings).

Exponential regression models were also tested for each forest type and treatment using the following equation: R_s (or CH_4 flux) = $a \times e^{(b \times \text{soil temperature})}$. Apparent thresholds in the R_s models near a soil temperature of 15 °C led to testing exponential regressions by splitting the data into 0–15 °C and 15–25 °C intervals (see Results section for more details). The Q_{10} value was then calculated for each R_s model using the equation: $Q_{10} = e^{(b \times 10)}$. These models were tested for the full range of soil temperatures as well as specific (limited) ranges. Statistics from the exponential regression models were produced from the residuals, which reflect the difference between predicted and observed values, following data linearization ($\ln(R_s) = \ln(a) + b \cdot$ soil temperature).

A series of multiple linear regressions were also tested to explain R_s and CH_4 fluxes (dependent variables). Soil temperature and soil water potential were always used as the first variable for the R_s and CH_4 models, respectively. Soil ionic activity (i.e., nitrogen ions, NO_3^- and NH_4^+, as well as PO_4^{3-} and Ca^{2+} ions), the presence or absence of conifers (binary variable where 0 = absence and 1 = presence), mostly balsam fir, as well as soil water potential (for R_s) and soil temperature (for CH_4) were tested as secondary explanatory variables for each forest type and stand in an attempt to explain variations in R_s and CH_4. As a means to test for non-linear relationships, the residuals of exponential regression models with soil temperature were also analyzed using different types of curvilinear regression models with residuals as the dependent variable and soil water potential or other variables as the independent variable.

To account for spatial and temporal variability of R_s within stands, the difference in R_s between spatial and temporal controls (ΔR_s) was calculated for all samplings in 2019 and 2020 within each stand, and ΔR_s was also calculated as the difference between spatial controls and heated plots for all samplings in 2021 and 2022. Both sets of ΔR_s were then plotted against R_s in the two controls (temporal for 2019 and 2020; spatial for 2021 and 2022) within each stand. As indicated previously, the absence of calibrated CH_4 data in 2019 and 2020 prevented us to build similar plots for CH_4. A pre-warming (i.e., 2019 and 2020) median of ΔR_s close to zero was expected to confirm the robustness of the experimental design because all the plots within a stand should exhibit similar R_s values prior to artificial warming. However, during the warming period (i.e., 2021 and 2022), ΔR_s values and medians diverging from zero indicate a change in R_s due to artificial warming. Positive and negative ΔR_s values indicate that artificial warming leads to an increase and a decrease in R_s, respectively. For data during the warming period, we also used a two-step approach to investigate whether there was a threshold (or breaking point) in the scatter of ΔR_s values along the R_s gradient. First, we visually inspected for a breaking point and then calculated two medians in the scatter of data according to that threshold. Second, we calculated the sum of errors around the main median and compared it to the weighed sum of errors (based on the number of points) around the two medians. We also compared the sum of errors based on two more thresholds before the visual threshold using a 50 mg CO_2 m^{-2} h^{-1} increment, as well as two more thresholds after the visual threshold using the same increment. For

each stand, we selected the threshold with the largest decrease in the sum of errors and considered it was significant when the decrease was greater than 20%.

3 Results

For both the heated plots and the spatial controls, R_s rates in 2021 and 2022 followed a seasonal pattern with an increase from May to July–August, followed by a decrease until the end of the snow-free period in October–November (Fig. 2C). Soil respiration rates in the heated plots varied from as low as 36.8 mg CO_2 m^{-2} h^{-1} in hardwood-beech stands in May 2022 (Fig. 4C) to as high as 791 mg CO_2 m^{-2} h^{-1} in mixedwoods in July 2022 (Fig. 4A). Methane fluxes exhibited no seasonal trend (Fig. 2D). Fluxes in CH_4 ranged for the most part (88%) between − 0.05 and − 0.25 mg CH_4 m^{-2} h^{-1} throughout the snow-free period (Fig. S1). The full CH_4 flux range was from 0.06 to − 0.39 mg CH_4 m^{-2} h^{-1}.

Two-way ANOVAs detected no significant treatment effect on R_s when all data, across all soil temperatures (0–25 °C), were considered. However, this was different when soil temperature intervals were considered, namely the 0–15 °C and 15–25 °C intervals (Table 2). Artificial soil warming yielded higher R_s only when considering the 0–15 °C interval, whereas for the forest type, the effect on R_s was significant only when considering the 15–25 °C interval. Two-way ANOVA also showed a significance of the interaction term (treatment × forest type) on R_s, but only when considering the whole temperature range (Table 2). Among all soil temperature intervals tested, the 0–15 °C and 15–25 °C intervals were the main intervals for which significant differences between treatments were found for R_s. See the Discussion section for a full rationale about this temperature (i.e., 15 °C) threshold.

No significant effect of treatment and forest type, nor a significant interaction between the two variables, was detected for CH_4 (Table 2; Fig. 3). Furthermore, CH_4 was not linearly or exponentially related to either soil water potential or soil temperature, nor with secondary variables such as soil ionic activity or conifer presence (Fig. S1).

The seasonal variation in R_s (Fig. 2C) followed a pattern similar to that of soil temperature (Fig. 2B). The determination coefficients (R^2) of the exponential regression models between R_s and soil temperature for the heated plots and spatial controls of the three forest types (Figs. 4; 5) were relatively low, ranging between 0.30 and 0.45, but statistically significant ($P < 0.05$, Table 3). The Q_{10} values of the regression models varied from 1.85 for heated plots and spatial controls of hardwoods to 3.28 for spatial controls of hardwood-beech stands. Furthermore, Q_{10} values were higher for spatial controls than for heated plots in mixedwoods and hardwood-beech stands, whereas they were identical between spatial controls and heated plots in hardwoods (Table 3). Soil respiration rates were generally highest in mixedwoods and lowest in hardwood-beech stands, except for spatial controls of hardwood-beech stands where R_s exceeded that of hardwoods starting at a soil temperature of about 14 °C (Fig. 4). None of the secondary variables (e.g., soil water potential, soil solution ionic activity, conifer presence) improved the prediction of R_s (results not shown).

The overlay of the regression curves from 2019–2020 and 2021–2022 demonstrated different responses of R_s to warming based on forest type (Fig. 5). For hardwood-beech stands, R_s in heated plots was lower than that in spatial and temporal controls starting at a 10–12 °C threshold, and this difference largely increased with increasing soil temperatures (Fig. 5C). For mixedwoods, a similar pattern was observed but the soil temperature threshold was shifted by about 2 °C (12–14 °C) and the difference between heated plots and spatial controls was marginal (Fig. 5A). For hardwoods, R_s in heated plots fell below that in spatial controls throughout the whole soil temperature range, although the difference was again marginal (Fig. 5B).

Plotting ΔR_s against R_s in control plots shows that the effect of artificial warming on R_s not only varied between forest types but also between stands (Fig. 6; Fig. S2-S6). For the pre-warming period (i.e., 2019 and 2020), ΔR_s values and medians were around 0 mg CO_2 m^{-2} h^{-1} for most of the stands, except stands 4 (positive) and 8 (negative). A pre-warming median of ΔR_s close to zero was expected and confirms the robustness of the experimental design (i.e., before the onset of warming, R_s in heated plots was higher than that in control plots). However, ΔR_s values and medians for the warming period (i.e., 2021 and 2022) in all stands except stands 1 and 3 diverged from those during pre-warming, suggesting a change in R_s due to artificial warming. Positive responses were observed in stands 4, 6, 7 and 8, whereas negative responses were observed in stands 2, 5 and 7 (Fig. 6; Fig. S2-S6).

A break in the scatter of ΔR_s values was observed at R_s rates in spatial controls between 300 and 500 mg CO_2 m^{-2} h^{-1} (Fig. 6; Fig. S2-S6; Table 4). We identified five out of eight stands (i.e., 2, 4, 5, 7 and 8) for which the sum of errors of ΔR_s values around the main median was decreased by more than 20% when calculating two medians at these thresholds (Table 4). This pattern indicates that R_s in heated plots was higher (stands 4, 7 and 8) than or similar (stands 2 and 5) to

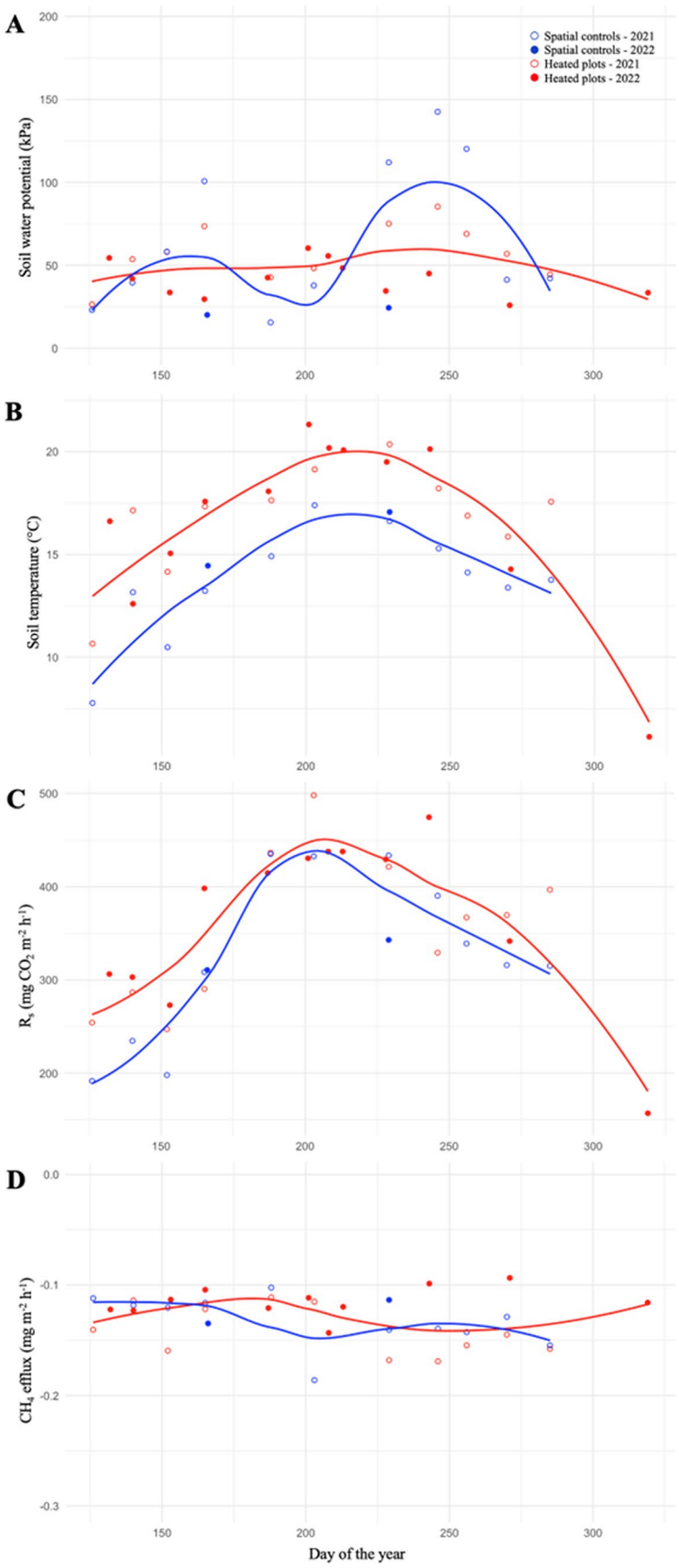


Fig. 2 Seasonal variations in soil water potential (**A**), soil temperature (**B**), soil respiration rates (R_s, **C**) and CH_4 fluxes (**D**) for the heated plots and spatial controls in 2021 and 2022. The red and blue data points represent the average of the heated plots and spatial controls, respectively, for each sampling in 2021 and 2022. The 2021 and 2022 data are represented by open and full circles, respectively. The lines were drawn with a smoothing function

Table 2 Significance levels of two-way ANOVAs to test the effect of treatment and forest type (and their interaction) on soil respiration rates (R_s) and CH_4 fluxes

Test	[0–15]°C	[15–25]°C	[0–25]°C
R_s			
Treatment	**	/	/
Forest type	*	***	***
Treatment × Forest type	/	/	*
CH_4			
Treatment	/	/	/
Forest type	/	/	/
Treatment × Forest type	/	/	/

p-value < 0.01 is indicated by *, < 0.001 by ** and < 0.001 by ***. The symbol / indicates a nonsignificant result (p > 0.05)

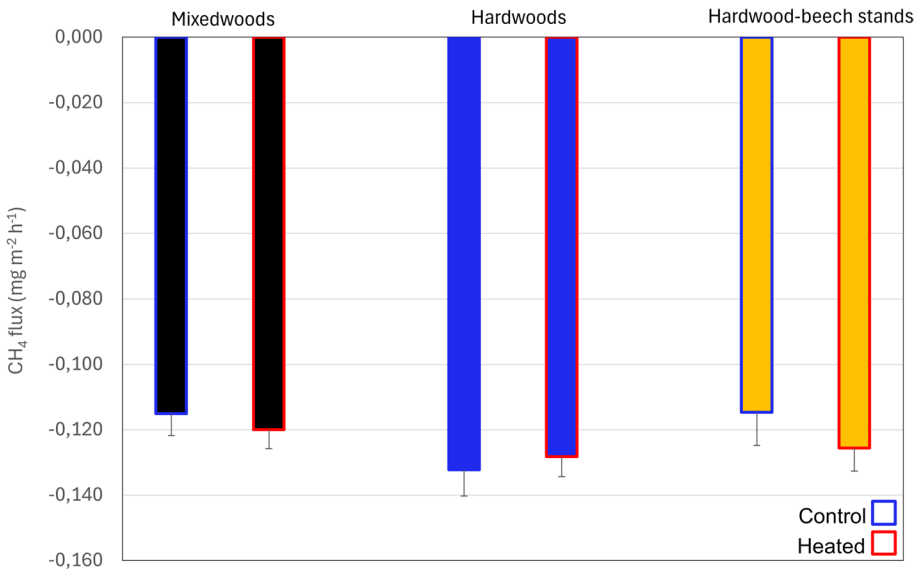


Fig. 3 Mean soil CH_4 flux in 2021 and 2022 under the heated plots (red contour) and spatial controls (blue contour) in mixedwoods (black), hardwoods (blue) and hardwood-beech stands (yellow). Bars are standard errors of the means. Two-way ANOVA detected no effect of treatment and forest type (and interactions) on CH_4

that in spatial controls and pre-warming levels below the 300–500 mg CO_2 m^{-2} h^{-1} thresholds, whereas R_s in heated plots was either lower (stands 2, 5 and 7) than or similar (stands 4 and 8) to that in spatial controls and pre-warming levels above these thresholds (Fig. 6; Fig. S2-S6; Table 4). For stands 3 and 6, these thresholds were not recognized as significant using our method (i.e., the decrease in the sum of errors was not > 20%, Table 4), whereas there was no apparent threshold for stand 1. Stands 5, 7 and 8 exhibited the lowest thresholds at 350, 350 and 300 mg CO_2 m^{-2} h^{-1}, two of which are hardwood-beech stands. However, because all forest types exhibited relatively similar thresholds in the scatter of ΔR_s during warming, it could not be clearly asserted that the break was associated to a specific forest type. The R_s thresholds correspond to a range in soil temperatures of approximately 12 to 18 °C in spatial controls (Fig. 4).

As indicated above, the sensitivity of R_s to soil temperature appeared to decrease from 12 to 18 °C, depending on the stand. A second series of exponential regressions was thus performed considering a soil temperature cutoff of 15 °C (i.e., the center of the 12–18 °C range). For the 0 to 15 °C range, the determination coefficients of the exponential relationships between soil temperature and R_s varied from 0.16 to 0.65 and models were statistically significant, whereas the coefficients for the 15–25 °C range were between 0.01 and 0.13 and models were mostly not significant (Table 5). As a reminder, two-way ANOVA results supported this 15 °C cutoff observed in the regressions based on a significant treatment effect on R_s for the 0–15 °C interval but not for the 15–25 °C interval.

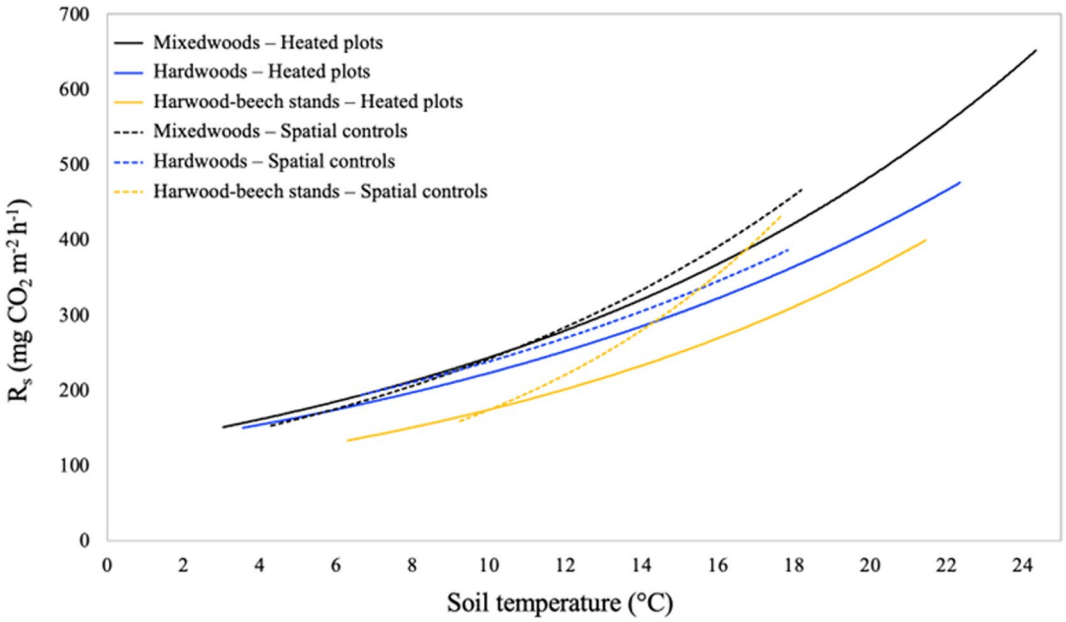


Fig. 4 Exponential relationships between soil temperature and soil respiration rates (R_s) for heated plots and spatial controls (2021 and 2022) in mixedwoods (black), hardwoods (blue) and hardwood-beech stands (yellow). Heated plots are presented as solid lines, whereas spatial controls are presented as dashed lines. See Table 3 for details on models and statistics. Data points are shown in Fig. 5

4 Discussion

4.1 Influence of soil water, artificial warming and other factors on CH_4 fluxes

Forest soils in this study are sandy and mostly located in upland positions and are thus well-drained throughout the snow-free period. Even during spring snowmelt, the soils drain rapidly and thus, they do not accumulate much moisture at any time [33, 51]. As such, aerobic methanotrophic bacteria consume CH_4 in such sandy upland soils and explain the consistent CH_4 sink measured during the snow-free period studied here (Figs. 2D, 3) and in other well-drained sandy to sandy loam forest soils [35, 36]. The sink is relatively large and compares to some literature reporting CH_4 fluxes for similar forest soils, e.g., [62]. Although methanotrophy is also influenced by soil temperature which affects bacteria, the sensitivity of the CH_4 sink to artificial warming appeared very limited (or nonexistent) in this study. This is in accordance with the bulk of the literature which suggests that artificial soil warming either does not influence the CH_4 sink or increases it slightly [42]. For example, artificial soil warming of + 4 °C over 15 years in a forest (spruce-fir-beech) of the Austrian Alps did not impact the soil CH_4 sink [43]. Experimental warming of + 3.4 °C in forest soils in Minnesota led to no statistical change in CH_4 flux after 5 years [41]. In his latter case, however, warming slightly increased the CH_4 sink when soil moisture was not limiting, whereas warming had slightly decreased the sink when soil moisture was limiting. The response of bacteria can depend on particle size distribution which affects how soils conserve water under warming. The amount of precipitation received during warming can also influence bacteria response and the CH_4 sink [43]. Considering that the soil warming treatment in this study yields a 2 °C difference with the spatial controls and that it tends to dry the soils [51], it was expected that the CH_4 sink would be increased slightly, but no change was observed. Other factors were proposed to have a stronger influence on CH_4 fluxes than soil temperature, e.g., nitrogen mineralization and NH_4 activity in the soil solution and tree species composition which affects litter quality, microbial activity and nitrogen availability [43, 44]. Yet, we found no relationship between CH_4 fluxes and either soil solution nutrient availability (nitrogen, phosphorus or calcium) and acidity (aluminium) or forest type (Fig. S1), suggesting a very consistent CH_4 sink during the snow-free period despite variations in soil conditions associated to forest types and the warming treatment. However, whether the sink's strength is weakened in the long term due to periods of high moisture under climate change deserves more attention at the study site [37, 43].

4.2 Effect of soil temperature and artificial warming on R_s

The increase in R_s observed in this study in response to artificial soil warming for the 0–15 °C interval (Table 3; Table 5) agrees with common knowledge that warmer soils generally lead to greater R_s in an array of ecosystems, and that soil temperature is the abiotic variable that exerts the greatest control over spatiotemporal variations in R_s [3, 6–8]. The observed increase in R_s in response to artificial soil warming also corroborates with the meta-analysis by Carey et al. [22] which suggests a positive effect of artificial warming on R_s across several ecosystems. Specifically for temperate forests, previous studies highlighted a strong positive curvilinear relationship between R_s and soil temperature, under either natural conditions [9, 11, 15, 62] or artificial warming [10, 63–65].

Although the relationship between R_s and soil temperature were significant for both spatial controls and heated plots of the three forest types, exponential regression models only explained 30–39% of the variability in R_s in spatial controls and 35 to 45% of the variability in heated plots. In comparison, exponential models in Bélanger et al. [9], which used the same experimental design prior to artificial warming, were more robust, explaining 55–65% of the variability in R_s. The latter models were developed from data collected in all plots in 2019 and 2020 (i.e., temporal controls). On the one hand, the decrease in predictability of R_s based on soil temperature can be attributed to smaller sample sizes in 2021 and 2022 compared to 2019 and 2020 as well as the lower number of observations in spatial controls compared to heated plots in 2021 and 2022 (about half of the measurements). On the other hand, the threshold of 15 °C, beyond which a weakening of the influence of soil temperature on R_s was observed in the heated plots, may partly explain the lower coefficients of determination of exponential regression models that include the full range of measured soil temperature (i.e., from 0 to 25 °C). Indeed, for all forest types and treatments, exponential relationships between temperature and R_s were remarkably more statistically robust when considering a range from 0 to 15 °C compared to relationships within the range of 15 to 25 °C (Table 5). Similarly, the 0 to 15 °C interval was the only interval for which a significant increase in R_s was found due to artificial warming (no effect from 0 to 25 °C and from 15 to 25 °C, Table 2).

For many stands, R_s started to decline (downshift) under artificial warming when R_s in spatial controls reached a threshold from 300 to 500 mg CO_2 m^{-2} h^{-1}. Based on exponential regression models, this range in R_s values corresponded to a range of soil temperature from 12 to 18 °C, with a median of 15 °C. As such, all results (i.e. ANOVAs, exponential regressions) suggest that the downshift in R_s due to artificial warming occurred at a threshold of about 15 °C. For the mixedwoods and hardwood-beech stands, the lower Q_{10} values of the regression models in heated plots compared to spatial controls also illustrated a decrease in R_s sensitivity to higher temperatures due to artificial warming (Table 3). Soil temperatures produced by artificial warming in this study were not unusually high compared to other temperate hardwood stands in the literature, mainly because the study site is at the very northern limit of the temperate deciduous forest with generally cooler soils. However, the decrease in predictability in R_s at a higher temperature range with a threshold set at about 15 °C is not common in the literature. In their meta-analysis, Carey et al. [22] determined that R_s rates increase with increasing soil temperature up to a threshold of approximately 25 °C in both heated and non-heated plots, above which R_s rates showed a downshift. Previous studies that focused on the effect of artificial warming on R_s generally demonstrated a decrease in sensitivity (i.e., a decrease in Q_{10}) over the long term, after at least 5 years of experimentation, due to a combination of phenomena such as microbial thermal acclimation, reduction in labile carbon reserves and soil drying [10, 66, 67].

The weakening of the influence of temperature on R_s in response to artificial soil warming in this study could depend on the influence of several other climatic and environmental variables, such as water availability and forest type, and the interactions between them. We speculate that the downshift of R_s at a 300–500 mg CO_2 m^{-2} h^{-1} threshold (or a decrease in the robustness of exponential models above 15 °C) is due to increased evaporative demand and soil drying during artificial warming. Soil drying induced by artificial warming was shown to offset the dependence of R_s on soil temperature [68], and moist soils were shown to exhibit a greater increase in R_s than dry soils [69]. Indeed, R_s depends on the balance between temperature and soil water availability [19]. Microbial activity and R_s are at their optimum within a certain range of soil water content and can be reduced or inhibited when soil water content is too low or too high [1, 70, 71]. For well-drained forest soils such as those in this study, water deficits during very specific periods can modulate R_s and the measured CO_2 flux is no longer related to soil temperature [9, 15]. However, in this study, integrating soil water potential along with temperature into various multiple linear regression models did not improve the prediction of R_s in any stand. Even after dividing the database into "cold" and "warm" temperature intervals (i.e., either below or above 15 °C), soil temperature remained the main variable modulating R_s, despite a considerable weakening of the relationship above 15 °C. Overall, however, no statistical test performed could clearly demonstrate that soil water potential governed,

at least partially, R_s at the study site, not even under higher soil temperatures. This outcome does not imply that water availability does not influence R_s. Rather, it can mean that drought characteristics (i.e., frequency and intensity) were not entirely conducive to statistical testing with R_s, and/or that the effect of water availability may be confounded by other variables and processes that are a function of forest type and species composition.

At first glance, our results suggest that the magnitude of the positive feedback loop between climate warming and soil CO_2 emissions from forest ecosystems could be limited [8, 72], at least for Quebec temperate deciduous forests. However, before the effect of warming on R_s becomes limited by induced soil drying, R_s could increase in response to rising soil temperature and contribute to radiative forcing in these systems. Further monitoring of R_s under artificial warming is planned at the study site to verify these responses, and ideally, more sites with other species compositions should be tested for a better portrait of the bioclimatic domain in question.

4.3 Forest type influence on R_s response to artificial warming

The significant effect of forest type on R_s across all temperature intervals, although a stronger response for the 15–25 °C interval, demonstrates that the three forest types respond differently to artificial warming in regard to R_s (Table 2). Even though the results highlighted a common pattern between all three forest types, which is a weakening of the influence of temperature on R_s after 15 °C, we observed a greater downshift of R_s in response to warming in hardwood-beech stands. Indeed, the temperature threshold from which R_s of heated plot fell below that of spatial controls was lower than in mixedwoods and hardwoods (i.e. 10–12 °C). The Q_{10} values also illustrated this greater sensitivity decrease, since the difference between spatial controls and heated plots was more substantial (3.28 and 2.07 respectively). This difference in R_s response to warming between the three forest types could be attributed to species-specific behaviors in response to changes in hydroclimatic conditions induced by artificial warming.

In terms of water potential, although there are annual and seasonal variations, soils in mixedwoods are generally the driest at the study site, whereas soils in hardwood-beech stands are the wettest [33]. In 2022, for example, hardwoods were generally wetter than hardwood-beech stands (results not shown), unlike the previous five years monitored. For both 2021 and 2022, soil water potential was higher in heated plots than spatial controls for all three forest types, except during the peak of summer (i.e., July) where the opposite was observed (shown for 2022 in Fig. 7). These results are counterintuitive since it was initially hypothesized that artificial warming would accentuate the drought conditions in heated plots during the warmest months due to increased evaporative demand. This pattern was further apparent in hardwood-beech stands in 2022 because soil water potential was lower than in hardwoods in July, while it was generally between that of mixedwoods and hardwoods otherwise (Fig. 7). All three forest types appeared to exhibit a behavior that limits water loss in warmer and drier conditions (i.e., heated plots), but this behavior seemed even more pronounced in hardwood-beech stands in 2022. We hypothesized that this ability of hardwood-beech stands to better conserve water could be explained by the isohydric behavior of beech spp. [33], and that this water-use strategy could partly explain the more significant downshift of R_s observed in this forest type in response to warming.

Across species, stomatal control to regulate water use is often described along a continuum from isohydry to anisohydry [73]. In periods of water stress, isohydric species tend to close their stomata, which decreases CO_2 assimilation, photosynthesis and productivity, but limits transpiration losses. On the other hand, anisohydric species keep their stomata open, which maintains gas exchanges and leads to a greater water loss [73]. While the literature has often emphasized the anisohydric behavior of beech spp., Courcot et al. [33] suggested that beech had an isohydric behavior that more efficiently resisted soil drying at the study site. Indeed, soils in hardwood-beech stands shifted to a "very high" state of water potential (> 120 kPa) at a soil temperature of 15.9 °C compared to 12.9 °C for soils in mixedwoods. Other studies showed that isohydric behavior can lead to a decrease in R_s. For example, to compensate for the decrease in CO_2 assimilation due to stomatal closure, there can be an upward transport of CO_2 through root water uptake, which decreases autotrophic respiration and consequently R_s [74]. A part of CO_2 derived from root respiration is dissolved in the soil solution and can apparently be transported from the roots to the leaves via the xylem stream [75]. This process may be accentuated during dry periods for isohydric species with strict stomatal regulation [74]. We hypothesized that this process could also

Fig. 5 Exponential relationship between soil temperature and soil respiration rates (R_s) for temporal controls (2019 and 2020) and heated plots and spatial controls (2021 and 2022) of mixedwoods (**A**, black), hardwoods (**B**, blue), and hardwood-beech stands (**C**, yellow). Temporal controls are presented as solid grey lines, heated plots are presented as solid lines and spatial controls are presented as dashed lines. See Bélanger et al. [9] for details on models and statistics for temporal controls and Table 3 for details on models and statistics for heated plots and spatial controls

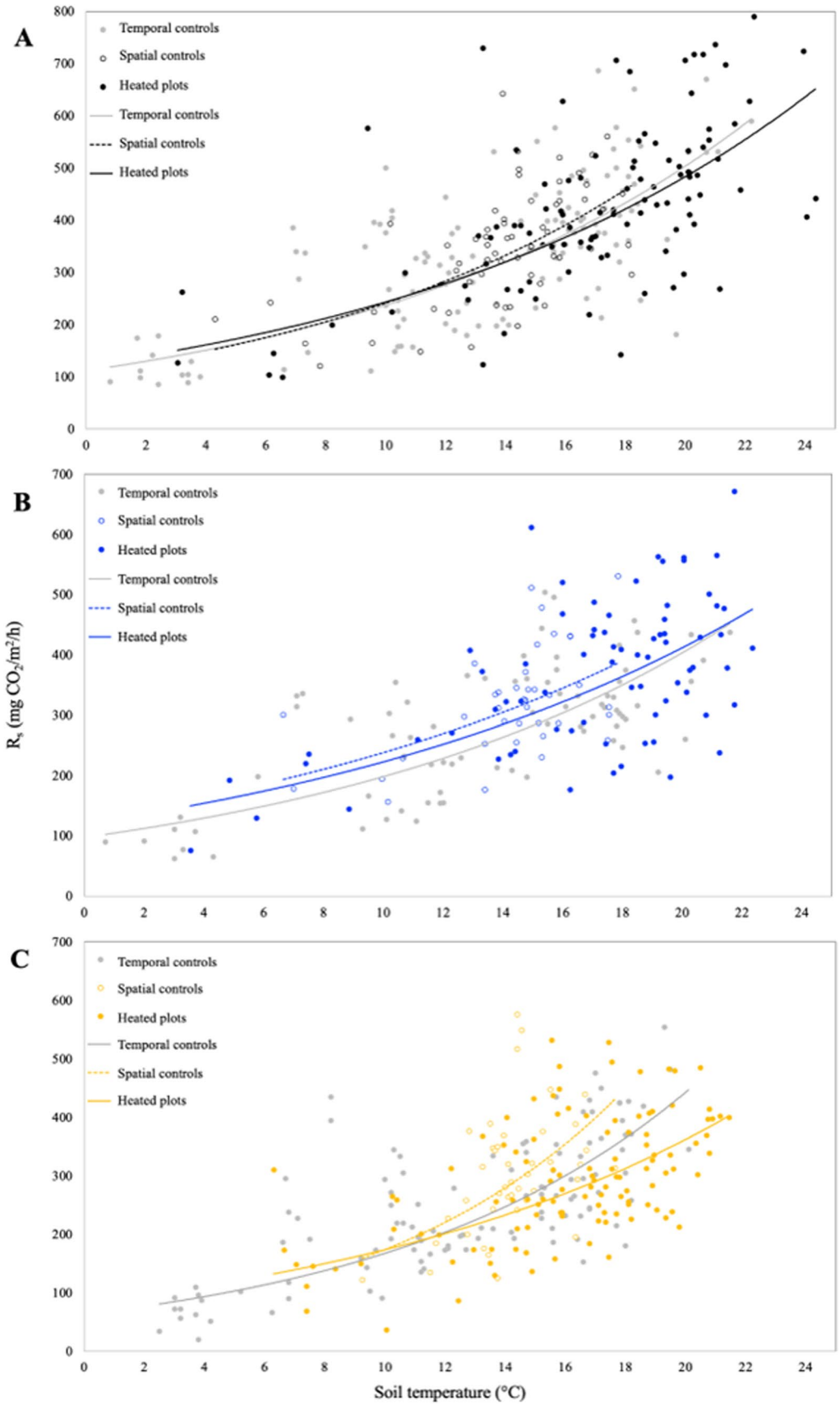

A
Temporal controls
Spatial controls
Heated plots
Temporal controls
Spatial controls
Heated plots
B
Temporal controls
Spatial controls
Heated plots
Temporal controls
Spatial controls
Heated plots
R_s (mg CO_2/m^2/h)
C
Temporal controls
Spatial controls
Heated plots
Temporal controls
Spatial controls
Heated plots
Soil temperature (°C)

Table 3 Parameters and Q_{10} values of exponential regression models between soil temperature and soil respiration rates (R_s) for heated and spatial controls (2021 and 2022) in mixedwoods, hardwoods and hardwood-beech stands

Forest type	Treatment	n	a	b	Q_{10}	R^2
Mixedwoods	Heated plots	101	122.4	0.0687	1.99	0.44*
	Spatial controls	61	108.3	0.0801	2.23	0.39*
Hardwoods	Heated plots	73	120.4	0.0615	1.85	0.45*
	Spatial controls	38	128.4	0.0617	1.85	0.30*
Hardwood-beech stands	Heated plots	112	84.2	0.0726	2.07	0.35*
	Spatial controls	42	53.0	0.1187	3.28	0.31*

p value < 0.05 is indicated by *

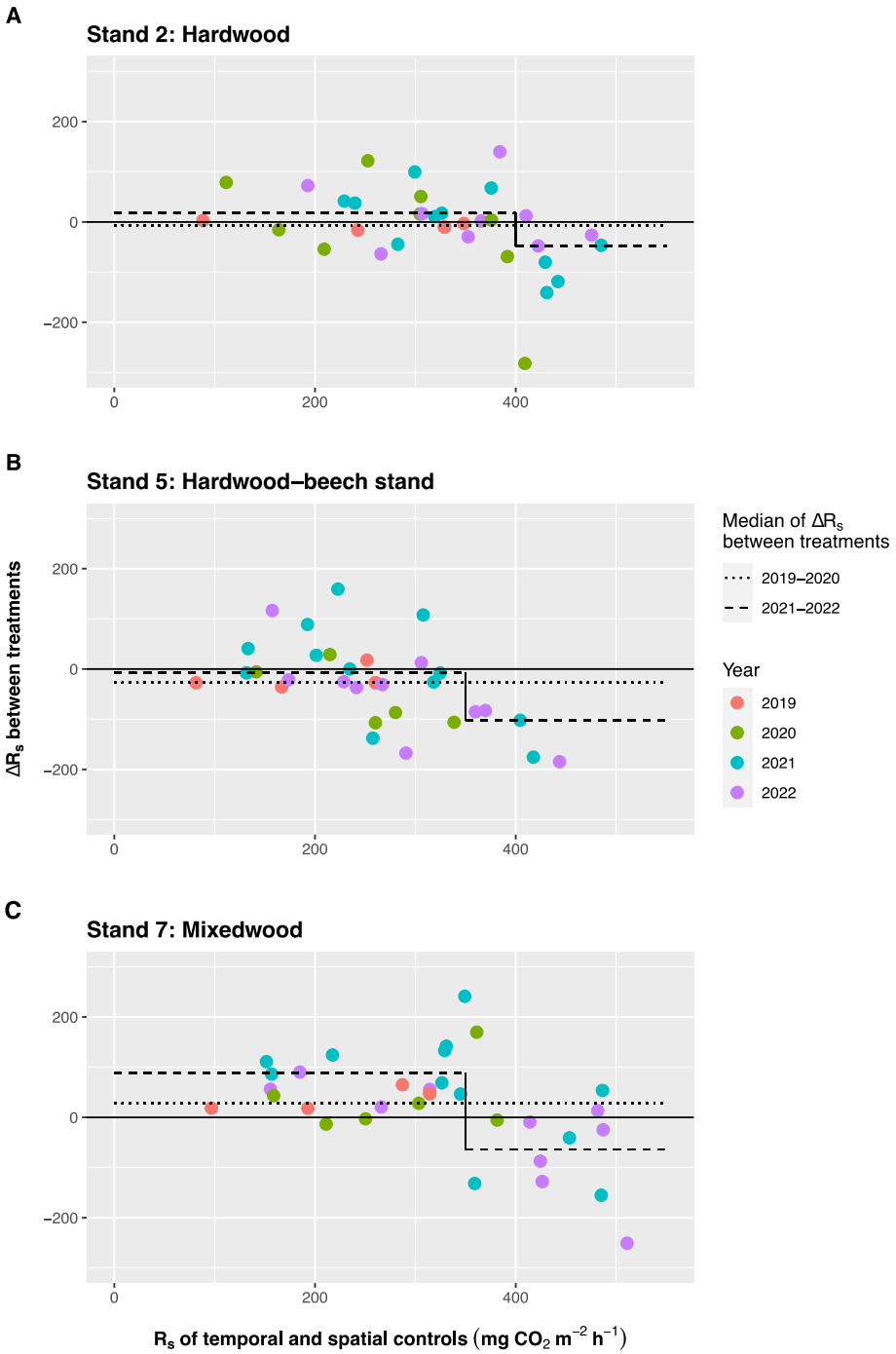


Fig. 6 Difference in soil respiration rates (R_s) between spatial and temporal controls (ΔR_s, pre-warming period in 2019 and 2020) as well as difference in R_s between heated plots and spatial controls (ΔR_s, warming period in 2021 and 2022) in stands 2 (**A**), 5 (**B**) and 7 (**C**), which are plotted against R_s of the two controls (temporal for 2019 and 2020; spatial for 2021 and 2022). Stand 2 is a hardwood, stand 5 is a hardwood-beech stand and stand 7 is a mixedwood. The ΔR_s medians during pre-warming were the closest to zero in these stands and thus, for the sake of clarity, they were the ones selected to exhibit R_s behavior. The years are represented by data points of different colors, while the two dashed lines represent the median of the two sets of ΔR_s (i.e., pre-warming and warming). Two medians were calculated for the warming dataset to highlight a threshold (or breaking point) in the scatter of ΔR_s values. Two medians instead of one decreased the sum of errors by more than 20% (Table 4). Data scatters for other stands are shown in supplementary materials (Fig. S2-S6)

Table 4 Selected threshold (breaking point) in the scatter of soil respiration (R_s, mg CO_2 m^{-2} h^{-1}) responses in each stand during artificial soil warming (Fig. 6; Fig. S2-S6) and percent decrease in the sum of errors when calculating two medians according to that threshold instead of just one median

Test	Stand	R_s threshold* mg CO_2 m^{-2} h^{-1}	Decrease in sum of errors %
Mixedwoods	1	NA	NA
	4	500	22,8
	7	350	34,4
Hardwoods	2	400	23,8
	6	400	10,3
Hardwood-beech stands	3	450	9,95
	5	350	23,6
	8	300	30,2

See Methods section for more details on calculations of medians and errors

*Spatial controls (2021 and 2022 data) are used as the R_s reference. NA means that no threshold was apparent and thus tested

Table 5 Parameters of exponential regression models between soil temperature and soil respiration rates (R_s) for the 0–15 °C and 15–25 °C intervals in heated and spatial controls (2021 and 2022) in mixedwoods, hardwoods and hardwood-beech stands

Forest type	Treatment	[0–15]°C		[15–25]°C	
		n	R^2	n	R^2
Mixedwoods	Heated plots	27	0.29*	74	0.14*
	Spatial controls	41	0.31*	020	0.01
Hardwoods	Heated plots	18	0.65*	55	0.06
	Spatial controls	22	0.32*	16	0.01
Hardwood-beech stands	Heated plots	36	0.16*	76	0.06*
	Spatial controls	32	0.35*	10	0.04

p value < 0.05 is indicated by *

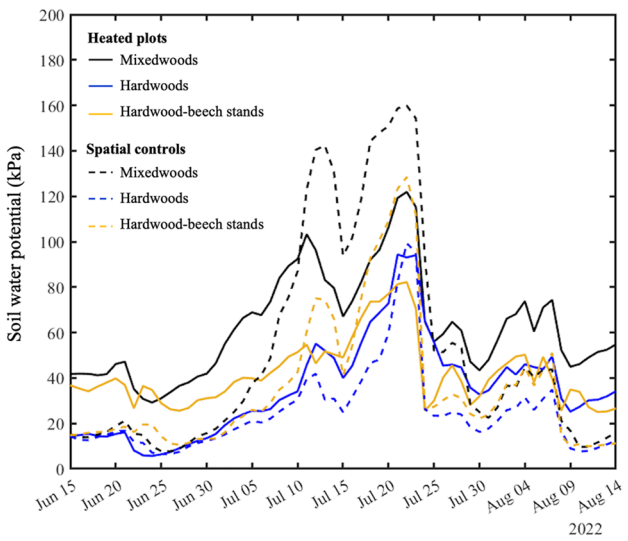


Fig. 7 Seasonal variations of soil water potential in heated plots (solid lines) and spatial controls (dashed lines) of mixedwoods (black), hardwoods (blue) and hardwood-beech stands (yellow) from mid-June to mid-August 2022

be active with beech at the study site, and thus this could partly explain the more important downshift of R_s in respect to increasing soil temperatures in heated plots of hardwood-beech stands compared to mixedwoods and hardwood stands. This is speculation and only the measurement of some proxies of this process (e.g., sapflow or dissolved CO_2 in the xylem) can confirm the hypothesis of CO_2 upward transport from roots to leaves in beech trees.

While we initially hypothesized that beech drought resistance demonstrated by Courcot et al. [33] would result in a smaller impact on R_s, we believe that the more obvious downshift of R_s in response to artificial warming observed

in hardwood-beech stands may result from the mechanisms enabling beech to adapt to water stress (e.g., stomatal closure). The species composing mixedwoods and hardwood stands also appeared to show a certain resistance to soil drying (i.e., lower soil water potential in the heated plots than in the spatial controls in the peak of summer), but this did not lead to a significant impact on R_s, unlike in hardwood-beech stands. The influence of this resistance and/or acclimatation to dryer conditions on R_s remains unclear, underscoring the importance, in the context of climate change and as a means to understand the overall role of forests on atmospheric CO_2, of augmenting studies focusing on the response of R_s under various forest types. Thus, further monitoring of soil water potential at the study site will provide a more robust representation of its complex behavior, which then can lead to stronger inferences and statistical models about the role of soil water on R_s under warming.

5 Conclusions

We studied R_s and CH_4 under a 2 °C artificial soil warming treatment in a temperate deciduous forest at its northern limit, where the abundance of conifers and American beech varied across the study site. The soil CH_4 sink did not change under warming during the snow-free period, whereas R_s increased in response to artificial warming, but only up to a threshold of about 15 °C, beyond which there was a downshift in R_s and the relationship between R_s and soil temperature was significantly weaker. On the one hand, as in other studies, methanotrophy was shown to be quite insensitive in the short term to artificial warming in well-drained upland forest soils. It was also consistent across forest types. On the other hand, the weakening of the soil temperature's influence on R_s after reaching a certain temperature was associated with augmented evaporative demand and thus soil drying induced by the treatment, although it could not be demonstrated statistically, likely due to complex species-specific behaviors in response to changes in hydroclimatic conditions. Contrary to our initial hypothesis, hardwood-beech stands were the most responsive to artificial warming and drying, which resulted in a more obvious downshift of R_s from a threshold of about 10–12 °C, even though it was the wettest forest type. The greater sensitivity in terms of R_s in hardwood-beech stands is possibly due to the isohydric behavior of beech during water stress, which limits root respiration (autotrophic) due to the upward transport of CO_2 to compensate for reduced gas exchange. The results of this study demonstrate the species-specific response to changes in soil hydroclimatic conditions in regard to R_s, which complexifies the study of the impact of a predicted rise in temperatures and decrease in soil water content on R_s. To adapt forests for optimal climate change mitigation, our results suggests that a better understanding of the relationship between species composition, soil hydroclimatic conditions and forest CO_2 cycle processes, such as R_s, is crucial. The long-term effects of soil warming and accompanying changes in soil hydroclimatic and biotic conditions on the CH_4 sink should also be more thoroughly studied for a full assessment of how forest soils impact greenhouse gas emissions as a whole.

Acknowledgements We would like to thank Alexandre Collin for his help in setting up the experimental design, as well as Joannie Beaulne-Raymond, William Brais, Maude Giguère, Jeanne-Lapierre St-Michel, Simon Lebel-Desrosiers et Joseph Mino-Roy for their help with sampling of gas fluxes. We would also like to thank the staff at SBL for providing access to the site and for hosting us during our visits.

Author contributions Conceptualization: N.B.; methodology, data curation and laboratory analysis: S.L., B.C., N.B. and R.T.-P.; figures production: S.L., B.C., N.B. and R.T.-P.; writing—original draft preparation, S.L and N.B..; writing—review and editing: S.L., B.C. and N.B.; funding acquisition: N.B. All authors have read and agreed to the published version of the manuscript.

Funding Financial support was provided to N. Bélanger by the Natural Sciences and Engineering Research Council of Canada (NSERC Discovery grants RGPIN 2015–03699 and 2020–04931 as well as several Undergraduate Research Awards), together with grants from the Canada Foundation for Innovation John R. Evans Leaders Fund (35370) and the Innovation Fund (36014, SmartForests Canada).

Data availability Available from corresponding author on request.

Code availability Not applicable.

Declarations

Competing interests The authors declare no competing interests.

Open Access This article is licensed under a Creative Commons Attribution-NonCommercial-NoDerivatives 4.0 International License, which permits any non-commercial use, sharing, distribution and reproduction in any medium or format, as long as you give appropriate credit to the original author(s) and the source, provide a link to the Creative Commons licence, and indicate if you modified the licensed material. You do not have permission under this licence to share adapted material derived from this article or parts of it. The images or other third party material in this article are included in the article's Creative Commons licence, unless indicated otherwise in a credit line to the material. If material is not included in the article's Creative Commons licence and your intended use is not permitted by statutory regulation or exceeds the permitted use, you will need to obtain permission directly from the copyright holder. To view a copy of this licence, visit http://creativecommons.org/licenses/by-nc-nd/4.0/.

References

1. Schlesinger WH. Biogeochemistry: an analysis of global change. 4th ed. Amsterdam: Elsevier; 2020.
2. Hanson PJ, Edwards NT, Garten CT, Andrews JA. Separating root and soil microbial contributions to soil respiration: a review of methods and observations. Biogeochemistry. 2000;48(1):115–46. https://doi.org/10.1023/A:1006244819642.
3. Kutsch W, Bahn M, Heinemeyer A. Soil carbon dynamics: an integrated methodology. Cambridge: Cambridge University Press; 2009.
4. Metcalfe DB, Fisher RA, Wardle DA. Plant communities as drivers of soil respiration: pathways, mechanisms, and significance for global change. Biogeosciences. 2011;8(8):2047–61. https://doi.org/10.5194/bg-8-2047-2011.
5. Raich JW, Tufekciogul A. Vegetation and soil respiration: correlations and controls. Biogeochemistry. 2000;48(1):71–90. https://doi.org/10.1023/A:1006112000616.
6. Davidson EA, Janssens IA. Temperature sensitivity of soil carbon decomposition and feedbacks to climate change. Nature. 2006;440(7081):165–73. https://doi.org/10.1038/nature04514.
7. Subke J-A, Bahn M. On the 'temperature sensitivity' of soil respiration: can we use the immeasurable to predict the unknown? Soil Biol Biochem. 2010;42(9):1653–6. https://doi.org/10.1016/j.soilbio.2010.05.026.
8. Schlesinger WH, Andrews JA. Soil respiration and the global carbon cycle. Biogeochemistry. 2000;48(1):7–20. https://doi.org/10.1023/A:1006247623877.
9. Bélanger N, Collin A, Khlifa R, Lebel-Desrosiers S. Balsam fir and American beech influence soil respiration rates in opposite directions in a sugar maple forest near its northern range limit. Front For Glob Change. 2021;4:664584. https://doi.org/10.3389/ffgc.2021.664584.
10. Melillo JM, Frey SD, DeAngelis KM, Werner WJ, Bernard MJ, Bowles FP, Pold G, Knorr MA, Grandy AS. Long-term pattern and magnitude of soil carbon feedback to the climate system in a warming world. Science. 2017;358(6359):101–5. https://doi.org/10.1126/science.aan2874.
11. Boone RD, Nadelhoffer KJ, Canary JD, Kaye JP. Roots exert a strong influence on the temperature sensitivity of soil respiration. Nature. 1998;396(6711):570–2. https://doi.org/10.1038/25119.
12. Moyano FE, Vasilyeva N, Bouckaert L, Cook F, Craine J, Curiel Yuste J, Don A, Epron D, Formanek P, Franzluebbers A, Ilstedt U, Kätterer T, Orchard V, Reichstein M, Rey A, Ruamps L, Subke J-A, Thomsen IK, Chenu C. The moisture response of soil heterotrophic respiration: interaction with soil properties. Biogeosciences. 2012;9(3):1173–82. https://doi.org/10.5194/bg-9-1173-2012.
13. Curiel Yuste J, Janssens IA, Carrara A, Ceulemans R. Annual Q_{10} of soil respiration reflects plant phenological patterns as well as temperature sensitivity. Glob Change Biol. 2004;10(2):161–9. https://doi.org/10.1111/j.1529-8817.2003.00727.x.
14. Giasson M-A, Ellison AM, Bowden RD, Crill PM, Davidson EA, Drake JE, Frey SD, Hadley JL, Lavine M, Melillo JM, Munger JW, Nadelhoffer KJ, Nicoll L, Ollinger SV, Savage KE, Steudler PA, Tang J, Varner RK, Wofsy SC, Foster DR, Finzi AC. Soil respiration in a northeastern US temperate forest: a 22-year synthesis. Ecosphere. 2013;4(11):1–28. https://doi.org/10.1890/ES13.00183.1.
15. Davidson EA, Belk E, Boone RD. Soil water content and temperature as independent or confounded factors controlling soil respiration in a temperate mixed hardwood forest. Glob Change Biol. 1998;4(2):217–27. https://doi.org/10.1046/j.1365-2486.1998.00128.x.
16. Schindlbacher A, Wunderlich S, Borken W, Kitzler B, Zechmeister-Boltenstern S, Jandl R. Soil respiration under climate change: prolonged summer drought offsets soil warming effects. Glob Change Biol. 2012;18(7):2270–9. https://doi.org/10.1111/j.1365-2486.2012.02696.x.
17. Lu M, Zhou X, Yang Q, Li H, Luo Y, Fang C, Chen J, Yang X, Li B. Responses of ecosystem carbon cycle to experimental warming: a meta-analysis. Ecology. 2013;94(3):726–38. https://doi.org/10.1890/12-0279.1.
18. Sierra CA, Trumbore SE, Davidson EA, Vicca S, Janssens I. Sensitivity of decomposition rates of soil organic matter with respect to simultaneous changes in temperature and moisture. J Adv Model Earth Syst. 2015;7(1):335–56. https://doi.org/10.1002/2014MS000358.
19. Wang Y, Song C, Liu H, Wang S, Zeng H, Luo C, He J-S. Precipitation determines the magnitude and direction of interannual responses of soil respiration to experimental warming. Plant Soil. 2021;458(1–2):75–91. https://doi.org/10.1007/s11104-020-04438-y.
20. Gatti LV, Basso LS, Miller JB, Gloor M, Gatti Domingues L, Cassol HLG, Tejada G, Aragão LEOC, Nobre C, Peters W, Marani L, Arai E, Sanches AH, Corrêa SM, Anderson L, Von Randow C, Correia CSC, Crispim SP, Neves RAL. Amazonia as a carbon source linked to deforestation and climate change. Nature. 2021;595(7867):388–93. https://doi.org/10.1038/s41586-021-03629-6.
21. Zhao B, Zhuang Q, Shurpali N, Köster K, Berninger F, Pumpanen J. North American boreal forests are a large carbon source due to wildfires from 1986 to 2016. Sci Rep. 2021;11(1):7723. https://doi.org/10.1038/s41598-021-87343-3.
22. Carey JC, Tang J, Templer PH, Kroeger KD, Crowther TW, Burton AJ, Dukes JS, Emmett B, Frey SD, Heskel MA, Jiang L, Machmuller MB, Mohan J, Panetta AM, Reich PB, Reinsch S, Wang X, Allison SD, Bamminger C, Bridgham S, Collins SL, de Bato G, Eddy WC, Enquist BJ, Estiarte M, Harte J, Henderson A, Johnson BR, Steenberg Larsen K, Luo Y, Marhan S, Melillo JM, Penuelas J, Pfeifer-Meister L, Poll C, Rastetter E, Reinmann AB, Reynolds LL, Schmidt IK, Shaver GR, Strong AL, Suseela V, Tietema A. Temperature response of soil respiration largely unaltered with experimental warming. Proc Natl Acad Sci. 2016;113(48):13797–802. https://doi.org/10.1073/pnas.1605365113.
23. Wu Z, Dijkstra P, Koch GW, Peñuelas J, Hungate BA. Responses of terrestrial ecosystems to temperature and precipitation change: a meta-analysis of experimental manipulation. Glob Change Biol. 2011;17(2):927–42. https://doi.org/10.1111/j.1365-2486.2010.02302.x.

24. Lloret F, Jaime LA, Margalef-Marrase J, Pérez-Navarro MA, Batllori E. Short-term forest resilience after drought-induced die-off in Southwestern European forests. Sci Total Environ. 2022;806:150940. https://doi.org/10.1016/j.scitotenv.2021.150940.
25. Peng C, Ma Z, Lei X, Zhu Q, Chen H, Wang W, Liu S, Li W, Fang X, Zhou X. A drought-induced pervasive increase in tree mortality across Canada's boreal forests. Nat Clim Chang. 2011;1(9):467–71. https://doi.org/10.1038/nclimate1293.
26. Sánchez-Pinillos M, D'Orangeville L, Boulanger Y, Comeau P, Wang J, Taylor AR, Kneeshaw D. Sequential droughts: a silent trigger of boreal forest mortality. Glob Change Biol. 2022;28(2):542–56. https://doi.org/10.1111/gcb.15913.
27. Senf C, Buras A, Zang CS, Rammig A, Seidl R. Excess forest mortality is consistently linked to drought across Europe. Nat Commun. 2020;11(1):6200. https://doi.org/10.1038/s41467-020-19924-1.
28. Johnstone JF, Allen CD, Franklin JF, Frelich LE, Harvey BJ, Higuera PE, Mack MC, Meentemeyer RK, Metz MR, Perry GL, Schoennagel T, Turner MG. Changing disturbance regimes, ecological memory, and forest resilience. Front Ecol Environ. 2016;14(7):369–78. https://doi.org/10.1002/fee.1311.
29. Yao Y, Fu B, Liu Y, Li Y, Wang S, Zhan T, Wang Y, Gao D. Evaluation of ecosystem resilience to drought based on drought intensity and recovery time. Agric For Meteorol. 2022;314:108809. https://doi.org/10.1016/j.agrformet.2022.108809.
30. Hesse BD, Gebhardt T, Hafner BD, Hikino K, Reitsam A, Gigl M, Dawid C, Häberle K-H, Grams TEE. Physiological recovery of tree water relations upon drought release—response of mature beech and spruce after five years of recurrent summer drought. Tree Physiol. 2023;43(4):522–38. https://doi.org/10.1093/treephys/tpac135.
31. De Soto L, Cailleret M, Sterck F, Jansen S, Kramer K, Robert EMR, Aakala T, Amoroso MM, Bigler C, Camarero JJ, Čufar K, Gea-Izquierdo G, Gillner S, Haavik LJ, Hereş A-M, Kane JM, Kharuk VI, Kitzberger T, Klein T, Levanic T, Linares JC, Mäkinen H, Oberhuber W, Papadopoulos A, Rohner B, Sanguesa-Barreda G, Stojanovic DB, Suarez ML, Villalba R, Martinez-Vilalta J. Low growth resilience to drought is related to future mortality risk in trees. Nat Commun. 2020;11(1):545. https://doi.org/10.1038/s41467-020-14300-5.
32. Kannenberg SA, Schwalm CR, Anderegg WRL. Ghosts of the past: how drought legacy effects shape forest functioning and carbon cycling. Ecol Lett. 2020;23(5):891–901. https://doi.org/10.1111/ele.13485.
33. Courcot B, Lemire D, Bélanger N. Dynamics of soil water potential as a function of stand types in a temperate forest: emphasis on flash droughts. Geoderma Reg. 2024;38:e00850. https://doi.org/10.1016/j.geodrs.2024.e00850.
34. Canarini A, Schmidt H, Fuchslueger L, Martin V, Herbold CW, Zezula D, Gündler P, Hasibeder R, Jecmenica M, Bahn M, Richter A. Ecological memory of recurrent drought modifies soil processes via changes in soil microbial community. Nat Commun. 2021;12(1):5308. https://doi.org/10.1038/s41467-021-25675-4.
35. Castro MS, Steudler PA, Melillo JM, Aber JD, Bowden RD. Factors controlling atmospheric methane consumption by temperate forest soils. Glob Biogeochem Cycles. 1995;9(1):1–10. https://doi.org/10.1029/94GB02651.
36. Feng H, Guo J, Han M, Wang W, Peng C, Jin J, Song X, Yu S. A review of the mechanisms and controlling factors of methane dynamics in forest ecosystems. For Ecol Manage. 2020;455:117702. https://doi.org/10.1016/j.foreco.2019.117702.
37. Ni X, Groffman PM. Declines in methane uptake in forest soils. Proc Natl Acad Sci. 2018;115:8587–90. https://doi.org/10.1073/pnas.1807377115.
38. Gilliam FS, Burns DA, Driscol CT, Frey SD, Lovett GM, Watmough SA. Decreased atmospheric nitrogen deposition in eastern North America: predicted responses of forest ecosystems. Environ Pollut. 2019;244:560–74. https://doi.org/10.1016/j.envpol.2018.09.135.
39. Nisbet EG, Manning MR, Dlugokencky EJ, Englund Michel S, Lan X, Röckmann T, van der Denier Gon HAC, Schmitt J, Palmer PI, Dyonisius MN, Oh Y, Fisher RE, Lowry D, France JL, White JWC, Brailsford G, Bromley T. Atmospheric methane: comparison between methane's record in 2006–2022 and during glacial terminations. Glob Biogeochem Cycles. 2023. https://doi.org/10.1029/2023GB007875.
40. Yu L, Huang Y, Zhang W, Li R, Sun W. Methane uptake in global forest and grassland soils from 1981 to 2010. Sci Total Environ. 2017;607–608:1163–72. https://doi.org/10.1016/j.scitotenv.2017.07.082.
41. Martins CS, Nazaries L, Delgado-Baquerizo M, Macdonald CA, Anderson IC, Hobbie SE, Venterea RT, Reich PB, Singh BK. Identifying environmental drivers of greenhouse gas emissions under warming and reduced rainfall in boreal-temperate forests. Funct Ecol. 2017;31:2356–68. https://doi.org/10.1111/1365-2435.12928.
42. Yan W, Zhong Y, Yang J, Shangguan Z, Torn MS. Response of soil greenhouse gas fluxes to warming: a global meta-analysis of field studies. Geoderma. 2020;419:115865. https://doi.org/10.1016/j.geoderma.2022.115865.
43. Heinzle J, Kitzler B, Zechmeister-Boltenstern S, Tian Y, Kwatcho Kengdo S, Wanek W, Borken W, Schindlbacher A. Soil CH_4 and N_2O response diminishes during decadal soil warming in a temperate mountain forest. Agric For Meteorol. 2023;329:109287. https://doi.org/10.1016/j.agrformet.2022.109287.
44. Gatica G, Fernandez ME, Juliarena MP, Gyenge J. Environmental and anthropogenic drivers of soil methane fluxes in forests: global patterns ad among-biomes differences. Glob Change Biol. 2020;26:6604–15. https://doi.org/10.1111/gcb.15331.
45. Saunois M, Martinez A, Poulter B, Zhang Z, Raymond P, Regnier P, Canadell JG, Jackson RB, Patra PK, Bousquet P, Ciais P, Dlugokencky EJ, Lan X, Allen GH, Bastviken D, Beerling DJ, Belikov DA, Blake DR, Castaldi S, Crippa M, Deemer BR, Dennison F, Etiope G, Gedney N, Höglund-Isaksson L, Holgerson MA, Hopcroft PO, Hugelius G, Ito A, Jain AK, Janardanan R, Johnson MS, Kleinen T, Krummel P, Lauerwald R, Li T, Liu X, McDonald KC, Melton JR, Mühle J, Müller J, Murguia-Flores F, Niwa Y, Noce S, Pan S, Parker RJ, Peng C, Ramonet M, Riley WJ, Rocher-Ros G, Rosentreter JA, Sasakawa M, Segers A, Smith SJ, Stanley EH, Thanwerdas J, Tian H, Tsuruta A, Tubiello FN, Weber TS, van der Werf G, Worthy DE, Xu Y, Yoshida Y, Zhang W, Zheng B, Zhu Q, Zhu Q, Zhuang Q. Global methane budget. 2024. Earth Sci Syst data Discuss. https://doi.org/10.5194/essd-2024-115.
46. Saucier J-P, Robitaille A, Grondin P. Cadre bioclimatique du Québec. In: Schlich W, editor. Manuel de foresterie, ordre des ingénieurs forestiers du Québec. Québec: MultiMondes; 2009. p. 186–205.
47. Savage, C. (2001). *Recolonisation Forestière Dans les Basses Laurentides au Sud du Domaine Climacique de L'érablière à Bouleau Jaune*. [master's thesis]. Montréal, QC: Université de Montréal.
48. Soil Classification Working Group. The Canadian system of soil classification. 3rd ed. Ottawa: Agriculture and Agri-Food Canada Publication and NRC Research Press; 1998.

49. Bélanger N, Holmden C, Courchesne F, Côté B, Hendershot WH. Constraining soil mineral weathering $^{87}Sr/^{86}Sr$ for calcium apportionment studies of a deciduous forest growing on soils developed from granitoid igneous rocks. Geoderma. 2012;185–186:84–96. https://doi.org/10.1016/j.geoderma.2012.03.024.
50. Aronson EL, McNulty SG. Appropriate experimental ecosystem warming methods by ecosystem, objective, and practicality. Agric For Meteorol. 2009;149(11):1791–9. https://doi.org/10.1016/j.agrformet.2009.06.007.
51. Bélanger N, Chaput-Richard C. Experimental warming of typically acidic and nutrient-poor boreal soils does not affect leaf-litter decomposition of temperate deciduous tree species. Soil Systems. 2023;7(1):14. https://doi.org/10.3390/soilsystems7010014.
52. McHale PJ, Mitchell MJ. Disturbance effects on soil solution chemistry due to heating cable installation. Biol Fertil Soils. 1996;22(1–2):40–4. https://doi.org/10.1007/BF00384430.
53. Rustad LE, Ivan J. Experimental soil warming effects on CO_2 and CH_4 flux from a low elevation spruce–fir forest soil in Maine, USA. Glob Change Biol. 1998;4(6):597–605. https://doi.org/10.1046/j.1365-2486.1998.00169.x.
54. Verburg PSJ, Van Loon WKP, Lükewille A. The CLIMEX soil-heating experiment: soil response after 2 years of treatment. Biol Fertil Soils. 1999;28(3):271–6. https://doi.org/10.1007/s003740050493.
55. Arias-Navarro C, Díaz-Pinés E, Kiese R, Rosenstock TS, Rufino MC, Stern D, Neufeldt H, Verchot LV, Butterbach-Bahl K. Gas pooling: a sampling technique to overcome spatial heterogeneity of soil carbon dioxide and nitrous oxide fluxes. Soil Biol Biochem. 2013;67:20–3. https://doi.org/10.1016/j.soilbio.2013.08.011.
56. Pedersen AR, Petersen SO, Schelde K. A comprehensive approach to soil-atmosphere trace-gas flux estimation with static chambers. Eur J Soil Sci. 2010;61(6):888–902. https://doi.org/10.1111/j.1365-2389.2010.01291.x.
57. Görres C-M, Kutzbach L, Elsgaard L. Comparative modeling of annual CO_2 flux of temperate peat soils under permanent grassland management. Agr Ecosyst Environ. 2014;186:64–76. https://doi.org/10.1016/j.agee.2014.01.014.
58. Kandel TP, Lærke PE, Elsgaard L. Effect of chamber enclosure time on soil respiration flux: a comparison of linear and non-linear flux calculation methods. Atmos Environ. 2016;141:245–54. https://doi.org/10.1016/j.atmosenv.2016.06.062.
59. Kutzbach L, Schneider J, Sachs T, Giebels M, Nykänen H, Shurpali NJ, Martikainen PJ, Alm J, Wilmking M. CO_2 flux determination by closed-chamber methods can be seriously biased by inappropriate application of linear regression. Biogeosciences. 2007;4(6):1005–25. https://doi.org/10.5194/bg-4-1005-2007.
60. Bilodeau-Gauthier S, Paré D, Messier C, Bélanger N. Root production of hybrid poplars and nitrogen mineralization improve following mounding of boreal Podzols. Can J For Res. 2013;43(12):1092–103. https://doi.org/10.1139/cjfr-2013-0338.
61. Hangs RD, Greer KJ, Sulewski CA. The effect of interspecific competition on conifer seedling growth and nitrogen availability measured using ion-exchange membranes. Can J For Res. 2004;34(3):754–61. https://doi.org/10.1139/x03-229.
62. Epron D, Farque L, Lucot É, Badot P-M. Soil CO_2 efflux in a beech forest: dependence on soil temperature and soil water content. Ann For Sci. 1999;56(3):221–6. https://doi.org/10.1051/forest:19990304.
63. Noh NJ, Kuribayashi M, Saitoh TM, Muraoka H. Different responses of soil, heterotrophic and autotrophic respirations to a 4-year soil warming experiment in a cool-temperate deciduous broadleaved forest in central Japan. Agric For Meteorol. 2017;247:560–70. https://doi.org/10.1016/j.agrformet.2017.09.002.
64. Schindlbacher A, Schnecker J, Takriti M, Borken W, Wanek W. Microbial physiology and soil CO_2 efflux after 9 years of soil warming in a temperate forest – no indications for thermal adaptations. Glob Change Biol. 2015;21(11):4265–77. https://doi.org/10.1111/gcb.12996.
65. Teramoto M, Liang N, Ishida S, Zeng J. Long-term stimulatory warming effect on soil heterotrophic respiration in a cool-temperate broad-leaved deciduous forest in northern Japan. J Geophys Res Biogeosci. 2018;123(4):1161–77. https://doi.org/10.1002/2018JG004432.
66. Kirschbaum MUF. Soil respiration under prolonged soil warming: are rate reductions caused by acclimation or substrate loss? Glob Change Biol. 2004;10(11):1870–7. https://doi.org/10.1111/j.1365-2486.2004.00852.x.
67. Knorr W, Prentice IC, House JI, Holland EA. Long-term sensitivity of soil carbon turnover to warming. Nature. 2005;433(7023):298–301. https://doi.org/10.1038/nature03226.
68. Wang X, Liu L, Piao S, Janssens IA, Tang J, Liu W, Chi Y, Wang J, Xu S. Soil respiration under climate warming: differential response of heterotrophic and autotrophic respiration. Glob Change Biol. 2014;20(10):3229–37. https://doi.org/10.1111/gcb.12620.
69. Liang G, Stefanski A, Eddy WC, Bermudez R, Montgomery RA, Hobbie SE, Rich RL, Reich PB. Soil respiration response to decade-long warming modulated by soil moisture in a boreal forest. Nat Geosci. 2024. https://doi.org/10.1038/s41561-024-01512-3.
70. Borken W, Savage K, Davidson EA, Trumbore SE. Effects of experimental drought on soil respiration and radiocarbon efflux from a temperate forest soil. Glob Change Biol. 2006;12(2):177–93. https://doi.org/10.1111/j.1365-2486.2005.001058.x.
71. Skopp J, Jawson MD, Doran JW. Steady-state aerobic microbial activity as a function of soil water content. Soil Sci Soc Am J. 1990;54(6):1619–25. https://doi.org/10.2136/sssaj1990.03615995005400060018x.
72. Raich JW, Schlesinger WH. The global carbon dioxide flux in soil respiration and its relationship to vegetation and climate. Tellus B: Chem Phys Meteorol. 1992;44(2):81–99. https://doi.org/10.3402/tellusb.v44i2.15428.
73. Chen Z, Li S, Wan X, Liu S. Strategies of tree species to adapt to drought from leaf stomatal regulation and stem embolism resistance to root properties. Front Plant Sci. 2022;13:926535. https://doi.org/10.3389/fpls.2022.926535.
74. Wang Y, Zhang C, Xiao X, Wu H, Zhang J. Water-use strategies and functional traits explain divergent linkages in physiological responses to simulated precipitation change. Sci Total Environ. 2024;908:168238. https://doi.org/10.1016/j.scitotenv.2023.168238.
75. Aubrey DP, Teskey RO. Root-derived CO_2 efflux via xylem stream rivals soil CO_2 efflux. New Phytol. 2009;184(1):35–40. https://doi.org/10.1111/j.1469-8137.2009.02971.x.

Publisher's Note Springer Nature remains neutral with regard to jurisdictional claims in published maps and institutional affiliations.